Polymer Chemistry

# Protein Aggregation Nucleated by Functionalized Dendritic Polyglycerols



| | |
|---|---|
| Journal: | *Polymer Chemistry* |
| Manuscript ID | PY-ART-05-2020-000667 |
| Article Type: | Paper |
| Date Submitted by the Author: | 06-May-2020 |
| Complete List of Authors: | Bernhard, Samuel; Montana State University, Department of Chemistry and Biochemistry<br>Fricke, Mackenzie; Montana State University, Department of Chemistry and Biochemistry<br>Haag, Rainer; Institut für Chemie und Biochemie, Freie Universität Berlin<br>Cloninger, Mary; Montana State University, Department of Chemistry and Biochemistry |
| | |

ARTICLE

# Protein Aggregation Nucleated by Functionalized Dendritic Polyglycerols

Received 00th January 20xx,
Accepted 00th January 20xx

DOI: 10.1039/x0xx00000x

Samuel P. Bernhard,[a] Mackenzie S. Fricke,[a] Rainer Haag[b] and Mary J. Cloninger*[a]†

Dendritic polyglycerols (dPGs) are emerging as important polymers for the study of biological processes due to their relatively low toxicity and excellent biocompatibility. The highly branched nature and high density of endgroups make the dPGs particularly attractive frameworks for the study of multivalent interactions such as multivalent protein-carbohydrate interactions. Here, we report the synthesis of a series of lactose functionalized dPGs with different hydrodynamic radii. A series of lactose functionalized dPGs bearing different densities of lactose functional groups was also synthesized. These lactose functionalized dPGs were used to study the templated aggregation of galectin-3, a galactoside binding protein that is overexpressed during many processes involved in cancer progression. Dynamic light scattering measurements revealed a direct correlation between the hydrodynamic radii of the lactose functionalized dPGs and the size of the galectin-3/lactose functionalized dPG aggregates formed upon mixing the lactose functionalized dPGs with galectin-3 in solution. These studies exposed the critical role of galectin-3's *N*-terminal domain in formation of galectin-3 multimers and also enabled comparisons of polymer templated aggregation using nonspecific interactions versus specific protein-carbohydrate binding interactions.

## Introduction

Dendritic polyglycerols (dPGs) are hyperbranched polymers with extensive branching and a high density of endgroups, which can be functionalized for a variety of applications.[1] dPGs, which are shown schematically in Fig. 1, are relatively easy to synthesize, often via one pot synthesis routes using glycidol. These hyperbranched polymers have been demonstrated to have relatively low toxicity and immunogenicity, excellent biocompatibility, and antifouling properties.[2-4] Because many therapeutic agents have relatively low aqueous solubility and may need to be shielded from their environment prior to reaching their intended target *in vivo*, dPGs are showing promise as nanocarrier drug delivery systems[5-7] and have also been labelled for fluorescence and radio imaging.[8]

Carbohydrate functionalized hyperbranched polymers have been reported for a variety of biomedical applications. Because multivalency is a governing principle of the biological interactions between proteins and carbohydrates,[9-12] glycopolymers such as glyco-dPGs show great promise for the study and mediation of many biologically relevant multivalent interactions. For example, mannose functionalized hyperbranched polyglycerols with variations in mannose density and polymer size were bound to Concanavalin A (Con A, a tetrameric mannose binding protein) to study binding cooperativity.[13] In addition, surface plasmon resonance studies revealed that mannose functionalized dPGs were effective multivalent inhibitors of Con A/mannose interactions.[14] Hyperbranched dendritic polyglycerols with a high degree of mannose functionalization were found to bind effectively to *S. aureus*. Antibacterial photodynamic therapy using mannose and zinc porphyrin co-functionalized hyperbranched polyglycerols was observed in PBS with this system.[15] Studies with sialic acid functionalized dPGs were performed to evaluate the effectiveness of these compounds as antiviral nanomaterials against influenza A virus cell binding. The degree of sialic acid functionalization and the size of the nanomaterial was found to be important for optimization of efficacy.[16] Hyperbranched glycopolymers bearing galactosides were found to be hemocompatible but still toxic to hepatocytes *in vitro*,[17] and hyperbranched polyglycerols bearing m-nitrophenyl α-galactoside endgroups showed good potency against Cholera Toxin B.[18] Mannose, N-acetylglucose, galactose, lactose, and fucose functionalized hyperbranched polyglycerols were studied in inhibition assays with selectins, carbohydrate binding cell adhesion molecules that are important mediators of inflammation. Binding of glycosylated polymers was moderate until they were sulfated; upon sulfation, high affinity binding to both L- and P-selectins was observed.[19] Low affinity binding prior to sulfation was partially attributed to the steric hindrance that was inherent for the reported system, which did not include a flexible linker between the polymer and the carbohydrate.[19]

[a] *Department of Chemistry and Biochemistry, Bozeman, MT, 59717, USA.*
[b] *Institut für Chemie und Biochemie, Freie Universität Berlin, Takustr. 3, 14195 Berlin, Germany.*

† Submitted for the auspicious occasion of Prof. Eric Anslyn's 60th birthday celebration.

Electronic Supplementary Information (ESI) available: Procedure for mass determination using SEC-HPLC, chromatograms, MS profiles, and NMRs of lactose functionalized dPGs. See DOI: 10.1039/x0xx00000x

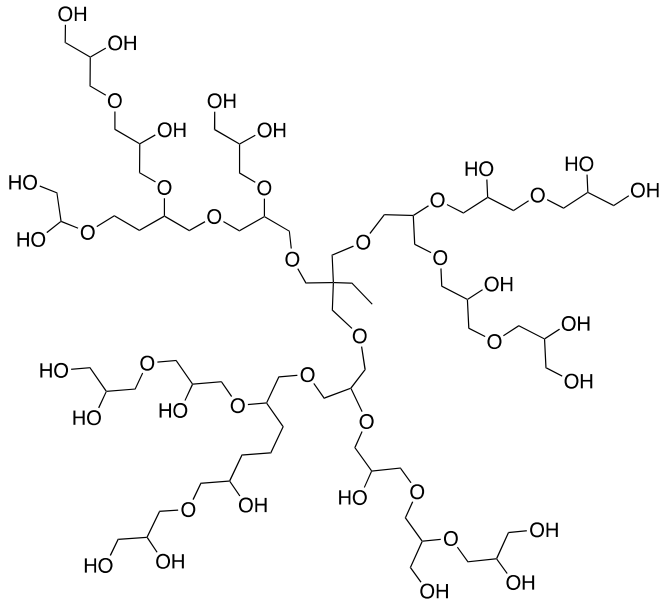

**Fig. 1** Schematic representation of the dPG framework.

Here, we report the synthesis and characterization of lactose functionalized dPGs (LdPGs) with an ethoxyethyl group linking the lactoside endgroups to the dPG frameworks. These compounds were synthesized in order to study the aggregation properties of galectin-3 and also to study galectin-3 mediated cancer cellular aggregation, an *in vitro* model for tumor formation. Galectin-3 is a β-galactoside binding protein that is overexpressed in many cancers and has a carbohydrate recognition domain with a shallow binding site specific for binding of galactosides.[20-23] In addition, an intrinsically disordered *N*-terminal, collagen-like domain is thought to induce aggregation of galectin-3 into multimeric forms during function.[24-27]

As described below, binding studies with lactose functionalized dPGs and galectin-3 using dynamic light scattering (DLS) reveal the importance of the hydrodynamic radii of the LdPGs in producing galectin-3 aggregates of reproducible and predictable sizes. Since the observed differences in cancer cellular aggregation correlate with the size differences of the galectin-3/LdPG aggregates, important conclusions regarding the requirements for galectin-3 aggregation during cancer cellular aggregation are drawn. As discussed below, the use of LdPGs to form aggregates of galectin-3 functionally simulates the interactions that occur for this protein's intrinsically disordered *N*-terminal domain at the cell surface during galectin-3 mediated cancer cellular aggregation.

## Experimental

**General Methods and Reagents.**

General reagents were purchased from Sigma Aldrich and Fisher chemical companies, and β-D-lactose (80% β) was purchased from Acros Organics. Unless stated, these reagents were used without any further purification. Dendritic polyglycerols were purchased from Nanopartica GmbH (Berlin, Germany) as a research kit containing dPGs with an average $M_n$ (number average molecular weight) of 1.48, 3.11, and 5.70 kDa and a polydispersity index (PDI) of 2.0, 1.6, and 1.4, respectively. Dialysis was carried out using Spectra/Por 6 regenerated cellulose tubing obtained from Spectrum Labs (Repligen Corp., Waltham, MA). Dry solvents were treated and obtained using a Meyer solvent system. $^1$H and $^{13}$C NMR spectra were recorded on a Bruker DPX 300 (300 and 75 MHz for $^1$H and $^{13}$C, respectively), a Bruker DRX 500 (500 and 126 MHz for $^1$H and $^{13}$C, respectively), and an AVANCE III Bruker 600 (600 and 151 MHz for $^1$H and $^{13}$C, respectively). NMR spectra are provided in the electronic supplementary information. LdPG products were evaluated by gel permeation chromatography using the Phenomenex GFC 4000 guard cartridge system followed by Waters Ultrahydrogel 500 and 250 columns and monitored at 235 nm with a Shimadzu SPD-M20A photodiode array. Sample injections (2.5 mg/mL, 100 µL) of lactoside functionalized PAMAM dendrimers, as calibration standards, and lactoside functionalized dPG were carried out in 250 mM aqueous KBr solution, at 40 °C, with a 1.0 mL/min flow rate. SEC-HPLC chromatograms and mass profiles are provided in the electronic supplementary information. Cellular aggregation assays were performed according to previously reported methods.[26, 27]

**4-O-(2,3,4,6-tetra-O-acetyl-β-D-galactopyranosyl) [1-4]-β-D-glucopyranose-tetra-O-1,2,3,6-acetate**

4-O-(β-D-galactopyranosyl)-β-D-glucopyranoside (100.00 g, 292 mmol) was suspended in acetic anhydride (300 mL, 3.17 mol, 10.9 equiv.). The reaction was cooled to 0 °C prior to addition of indium triflate (1.75 g, 3.10 mmol). The suspension was allowed to stir for 15 min until it was translucent and homogeneous. The reaction was allowed to return to room temperature, diluted to 1 L with ethyl acetate, and quenched with the slow addition of saturated aqueous $Na_2CO_3$ solution. The organic layer was collected and washed with $NaHCO_3$ (3 x 50 mL), water (3 x 50 mL) and brine (2 x 50 mL). The organic layer was dried over anhydrous $Na_2SO_4$, drying agent was removed by filtration, and the solution was concentrated to dryness. The resulting yellow oil was recrystallized (10:1 methanol/ $CH_2Cl_2$) in triplicate to obtain (139.18 g, 205 mmol, 70% yield) as a free-flowing white powder. $^1$H NMR (500 MHz, $CDCl_3$) δ 5.68 (d, J = 8.3 Hz, 1H, H1), 5.35 (d, J = 3.5 Hz, 1H, H4'), 5.25 (t, J = 9.2 Hz, 1H, H3), 5.11 (dd, J = 10.4, 7.9, 1H, H2'), 5.05 (t, J = 8.9 Hz, 1H, H2), 4.95 (dd, J = 10.4, 3.5 Hz, 1H, H3'), 4.48 (d, J = 7.9 Hz, 1H, H1'), 4.46 (dd, J = 12.2, 2.1 Hz, 1H, H6a), 4.16 - 4.06 (m, 3H, H6b, H6a', H6b'), 3.88 (t, J = 6.7 Hz, 1H, H5'), 3.85 (t, J = 9.4 Hz, 1H, H4) 3.77 (ddd, J = 10.0, 5.0, 2.1 Hz, 1H, H5), 2.16 (s, 3H, $CH_3$), 2.12 (s, 3H, $CH_3$) 2.10 (s, 3H, $CH_3$), 2.07 (s, 3H, $CH_3$), 2.06 (s, 3H, $CH_3$), 2.05 (s, 3H, $CH_3$), 2.03 (s, 3H, $CH_3$), 1.97 (s, 3H, $CH_3$). As reported.[28]

**4-O-(2,3,4,6-tetra-O-acetyl-β-D-galactopyranosyl) [1-4]-β-D-glucopyranose-tri-O-2,3,6-acetate (1).**

4-O-(2,3,4,6-tetra-O-acetyl-β-D-galactopyranosyl) [1-4]-β-D-glucopyranose-tetra-O-1,2,3,6-acetate (20.902 g, 3.1 mmol) was dissolved in dry DMF (150 mL) and allowed to stir over 4 Å

molecular sieves for 1 h. Hydrazine acetate (3.126 g, 3.4 mmol) was added, and the reaction was heated to 55 °C for 1 h, after which it was shown to be complete by TLC (1:4 EtOAc/$CH_2Cl_2$, ceric ammonium molybdate (CAM) stain–product is lower spot). The reaction was cooled to room temperature, extracted with $CH_2Cl_2$ and washed with sat. aq. $NaHCO_3$ solution (3 x 30 mL), water (3 x 30 mL) and brine (3 x 30 mL). The organic layer was dried over anhydrous $Na_2SO_4$, drying agent was removed by filtration, and the solution was concentrated to dryness *in vacuo* to give **1** as a white solid (16.679 g, 26.4 mmol, 86% yield). The crude material was used immediately in the next reaction. $^1$H NMR (500 MHz, $CDCl_3$) 5.50 (t, J = 9.7 Hz, 1H, H3α), 5.34 (d, J = 3.7 Hz, 1H, H1α), 5.32 (d, 1H, J = 3.4 Hz, H4'), 5.21 (t, J = 9.2 Hz, 1H, H3β), 5.11 - 5.05 (m, 2H, H2'α, H2'β), 4.94 (dd, J = 10.4, 3.5 Hz, 2H, H3'), 4.83 - 4.69 (m, 2H, H2α, H1β, H2β), 4.52 - 4.43 (m, 3H, H1'α, H6b, H1'β), 4.19 - 4.02 (m, 5H, H5, H6a, H6a', H6b'), 3.86 (t, J = 6.9 Hz, 2H, H5'), 3.81 - 3.62 (m, 2H, H4α), 2.13 (s, 3H, $CH_3$), 2.11 (s, 3H, $CH_3$) 2.05 (s, 3H, $CH_3$), 2.04 (s, 3H, $CH_3$ ), 2.03 (s, 3H, $CH_3$ ), 2.02 (s, 3H, $CH_3$ ), 1.94 (s, 3H, $CH_3$ ) ppm. As reported.[29]

**1-trichloroacetimidate-4-O -(2,3,4,6-tetra-O -acetyl-β-D-galactopyranosyl) [1-4]-β-D-glucopyranosyl-tri-O -2,3,6-acetate (2).**

Compound **1** (16.679 g, 26.4 mmol) was dissolved in $CH_2Cl_2$ (300 mL) and cooled to 0 °C. $Cl_3CCN$ (7.64 mL, 76 mmol) was added, followed by dropwise addition of 1,8-diazabicyclo[5.4.0]undec-7-ene (DBU, 551 µL, 3.7 mmol) under argon. The reaction was stirred at room temperature for 3 h and was monitored by TLC (1:4 EtOAc/$CH_2Cl_2$, CAM stain; product found above deprotected material). Once complete, the reaction was taken up in $CH_2Cl_2$ and washed with sat. aq. $NaHCO_3$ solution (1 x 30 mL), water (3 x 30 mL), brine (2 x 30 mL), and dried over $Na_2SO_4$. The drying agent was removed by filtration and the solvent was removed *in vacuo* to give **2** as a dark brown oil. Purification through a silica gel plug (1:4 EtOAc/$CH_2Cl_2$, CAM stain) afforded **2** (14.297 g, 18.3 mmol, 69% yield) as a white solid. $^1$H NMR (500 MHz, $CDCl_3$) δ 8.62 (s, 1H, NH), 6.40 (d, J = 3.8 Hz, 1H, H1α), 5.48 (t, J = 9.7 Hz, 1H, H3), 5.27 (d, J = 3.3 Hz, 1H, H4'), 5.04 (dd, J = 10.4, 7.9 Hz, 1H, H2), 4.98 (dd, J = 10.1, 3.9 Hz, 1H, H2'), 4.88 (dd, J = 10.4, 3.5 Hz, 1H, H3'), 4.48 - 4.38 (m, 2H, H6a, H1'), 4.11 - 3.98 (m, 4H, H5, H6b, H6a', H6b'), 3.85 - 3.77 (m, 2H, H4, H5'), 2.08 (s, 3H, $CH_3$), 2.03 (s, 3H, $CH_3$), 1.99 (s, 3H, $CH_3$), 1.99 (s, 3H, $CH_3$), 1.93 (s, 3H, $CH_3$), 1.89 (s, 3H, $CH_3$) ppm. As reported.[30]

**2-(2-azidoethoxy)ethanol (3).**

2-(2-chloroethoxy)ethanol (9.943 g, 79.8 mmol) and $NaN_3$ (12.97 g, 199.5 mmol, 2.5 equiv.) were dissolved in Millipore water (50 mL). The solution was allowed to stir for 32 h at 80 °C. The product was extracted with diethyl ether (3 x 100 mL) and dried *in vacuo* to afford 8.314 g of product **3** as a clear oil (62.0 mmol, 78% yield). $^1$H NMR (500 MHz, $CDCl_3$) δ 3.82 - 3.74 (m, 2H, $CH_2OH$), 3.72 (t, J = 5.0 Hz, 2H, $CH_2CH_2OH$), 3.64 (ddd, J = 5.3, 3.5, 1.4 Hz, 2H, $CH_2CH_2N_3$), 3.43 (t, J = 5.0 Hz, 2H, $CH_2N_3$), 2.18 (s, 1H, OH) ppm. $^{13}$C NMR (126 MHz, $CDCl_3$) δ 72.6, 70.3, 62.0, 51.0 ppm. As reported.[31]

**5-azido-3-oxopentyl-2,3,4,6-tetra-O-acetyl-β-D-galactopyranosyl [1-4]-2,3,6-tri-O-acetyl-β-D-glucopyranose (4).**

Lactose trichloroacetimidate **2** (4.040 g, 5.2 mmol) and 2-(2-azidoethoxy)ethanol **3** (0.834g, 6.4 mmol) were dissolved in dry $CH_2Cl_2$ (40 mL). The reaction was cooled to 0 °C prior to addition of indium triflate (0.15 g, 0.26 mmol); the clear yellow solution became opaque. The reaction was allowed to warm to room temperature where it stirred for 16 h, until complete by TLC (4:1 $CH_2Cl_2$/EtOAc, CAM stain). The reaction was quenched via slow addition of water and extracted with $CH_2Cl_2$ (3 x 20 mL). It was washed with water (3 x 10 mL) and brine (1 x 10 mL), and dried over anhydrous $Na_2SO_4$. The drying agent was removed by filtration, and the solvent was removed *in vacuo* to afford a yellow oil. The product was purified using silica gel with 1:3 EtOAc/hexane eluent, followed by recrystallization (10:1 methanol/$CH_2Cl_2$) to obtain product **4** as white crystalline solid (2.394 g, 0.00319 mol, 62% yield). $^1$H NMR (600 MHz, $CDCl_3$) δ 5.32 (dd, J = 3.5, 1.2 Hz, 1H, H4'), 5.18 (t, J = 9.3 Hz, 1H, H3), 5.09 (dd, J = 10.4, 7.9 Hz, 1H, H2'), 4.93 (dd, J = 10.4, 3.5 Hz, 1H, H3'), 4.88 (dd, J = 9.5, 7.9, 1H, H2), 4.55 (d, J = 7.9 Hz, 1H, H1'), 4.50 - 4.45 (m, 2H, H1, H6a), 4.15 - 4.02 (m, 3H, H6b, H6a', H6b'), 3.97 - 3.51 (m, 9H,-OCH*H*, H5', H4, OC*H*H, $OCH_2$, $CH_2O$, H5), 3.34 (t, J = 5.1 Hz, 2H, $CH_2N_3$), 2.13 (s, 3H, $CH_3$), 2.10 (s, 3H, $CH_3$), 2.04 (s, 3H, $CH_3$), 2.02 (s, 9H, $CH_3$), 1.94 (s, 3H, $CH_3$) ppm. $^{13}$C NMR (151 MHz, $CDCl_3$) δ 170.4, 170.3, 170.1, 170.1, 169.7, 169.7, 169.0, 101.1, 100.6, 76.2, 72.8, 72.6, 71.7, 71.0, 70.7, 70.4, 70.2, 69.1, 66.6, 62.0, 60.8, 50.8, 20.9, 20.8, 20.7, 20.7, 20.6, 20.5 ppm. As reported.[30]

**Dendritic polyglycerol propargyl ether 5.**

Stock 2.5 kDa dendritic polyglycerol (848 mg, 0.573 mmol) was dried under high vacuum for 72 h and dissolved in anhydrous DMF (5 mL). NaH, obtained as a 60% dispersion in mineral oil (336 mg, 8.4 mmol, was activated with hexanes (3 x 5 mL) and suspended in DMF. The reaction was cooled to 0 °C and the NaH suspension was added dropwise. The solution was slowly brought back to room temperature and stirred for 2 h. Reaction was again cooled to 0 °C, then propargyl bromide, obtained as an 80% solution in toluene (0.815 mL, 7.6 mmol), was added dropwise. The solution turned light brown as the reaction progressed for 72 h. The resulting product was quenched with 20 mL methanol and dialyzed against 1000 MWCO tubing in MeOH to obtain **5** as a viscous light brown oil (237 mg, 17% chemical yield). The product was dissolved in methanol and stored with BHT as a radical quencher. Spectra matched previously reported data.[32] $^1$H NMR (300 MHz, $CD_3OD$) δ 4.32 (ap. s, 36H, CH*H*CCH), 4.19 (ap. s, 24H, C*H*HCCH), 3.98 - 3.36 (m, 314H, dPG backbone), 2.87 (ap. s, 27H, CCH), 1.39 (ap. s, 2H, CH2, initiator), 0.88 (ap. s, 3H, initiator) ppm.

**Dendritic polyglycerol propargyl ether 6.**

Stock 5 kDa dendritic polyglycerol (863 mg, 0.277 mmol) was dried under high vacuum for 72 h, then dissolved in anhydrous DMF (5 mL). NaH, obtained as a 60% dispersion in mineral oil (345 mg, 8.6 mmol), was activated with hexanes (3 x 5 mL) and

suspended in DMF. The reaction was cooled to 0 °C, and the NaH suspension was added dropwise. The solution was slowly brought back to room temperature and stirred for 2 h. Reaction was again cooled to 0 °C, then propargyl bromide, obtained as an 80% solution in toluene (0.80 mL, 7.4 mmol), was added dropwise. The solution turned light brown as the reaction progressed for 72 h. The resulting product was quenched with 20 mL methanol and dialyzed against 1000 MWCO tubing in methanol to obtain **6** as a viscous light brown oil (431 mg, 31 % chemical yield). The product was dissolved in methanol and stored with BHT as a radical quencher. Spectra matched previously reported data.[32] $^1$H NMR (300 MHz, $CD_3OD$) δ 4.33 (ap. s, 46H, C*H*HCCH), 4.19 (ap. s, 36H, CH*H*CCH), 3.98 - 3.36 (m, 416H, dPG backbone), 2.88 (ap. s, 37, CCH), 1.40 (ap. s, 2H, $CH_2$, initiator), 0.89 (ap. s, 3H, $CH_3$, initiator) ppm.

**Dendritic polyglycerol propargyl ether 7.**

Stock 10 kDa dendritic polyglycerol (832 mg, 0.146 mmol) was dried under high vacuum for 72 h, then dissolved in anhydrous DMF (5 mL). NaH, obtained as a 60% dispersion in mineral oil (335 mg, 8.4 mmol), was activated with hexanes (3 x 5 mL) and suspended in DMF. The reaction was cooled to 0 °C and the NaH suspension was added dropwise. The solution was slowly brought back to room temperature and stirred for 2 h. Reaction was again cooled to 0 °C, then propargyl bromide, obtained as an 80% solution in toluene (0.82 mL, 7.6 mmol), was added dropwise. Solution turned to a light brown as the reaction progressed for 72 h. The resulting product was quenched with 20 mL methanol and dialyzed against 1000 MWCO tubing in $CH_3OH$ to obtain **7** as a viscous light brown oil (634 mg, 46% chemical yield). The product was dissolved in methanol and stored with BHT as a radical quencher. Spectra matched previously reported data.[32] $^1$H NMR (300 MHz, $CD_3OD$) δ 4.27 (ap. s, 58H, C*H*HCCH), 4.13 (ap. s, 45H, CH*H*CCH), 3.98 - 3.36 (m, 599H, dPG backbone), 2.83 (ap. s, 47H, CCH), 1.45 (ap. s, $CH_2$, initiator), 0.94 (ap. s, $CH_3$, initiator) ppm.

**Acetylated lactose functionalized dendritic polyglycerol 8.**

Dendritic polyglycerol propargyl ether **5** (2.64 kDa, 10 terminal alkynes), obtained as a butylated hydroxytoluene (BHT) stabilized solution in MeOH, was dried down (7 mg, 3 µmol) and reconstituted in 590 µL THF with lactose azide **4** (50 mg, 67 µmol, 2.4 equiv.). Sodium ascorbate (15 mg, 71 µmol) was introduced as a 145 µL aliquot from a 100 mg/mL aqueous solution. Copper (II) sulfate (4 mg, 18.0 µmol) was introduced as a 448 µL aliquot from a 10 mg/mL aqueous solution. The reaction was allowed to stir for 48 h prior to addition of a 600 µL aliquot of 20 mg/mL EDTA solution. After EDTA addition, the reaction was stirred for 1 h. Product was extracted with EtOAc (3 x 3 mL) and dried *in vacuo*. Product was dialyzed using 1000 MWCO tubing in DMSO with progress monitored by TLC (EtOAc, CAM stain) until small molecule spots were no longer observed with the polymer. The solvent was removed *in vacuo* to afford 48 mg of product **8** (84 % chemical yield) as an oil. $^1$H NMR (500 MHz, $CDCl_3$) δ 7.76 (bs, 1H, triazole), 5.36 (d, J = 3.5 Hz, 1H, H4'), 5.20 (t, J = 9.1 Hz, 1H, H3), 5.11 (t, J = 9.5 Hz, 1H, H2'), 4.98 (dd, J = 10.5, 3.6 Hz, 1H, H3'), 4.89 (t, J = 9.1 Hz, 1H, H2), 4.78 (bs, 1H), 4.68 (bs, 1H), 4.58-4.46 (ap. s, 5H), 4.11 - 3.98 (m, 3H), 3.97 - 3.76 (m, 5H), 3.73 - 3.42 (m, 10H, dPG backbone), 2.16 (s, 3H, $CH_3$), 2.12 (s, 3H, $CH_3$), 2.07 (s, 3H, $CH_3$), 2.06 (s, 6H, $CH_3$), 1.98 (s, 3H, $CH_3$), 1.27 (bs, 2H, $CH_2$, initiator), 0.85 (bs, 3H, $CH_3$, initiator) ppm. $^{13}$C NMR (126 MHz, $CDCl_3$) δ 170.3, 170.2, 169.8, 169.6, 169.1, 101.0, 100.6, 76.2, 72.7, 71.6, 71.0, 70.6, 70.1, 69.5, 69.1, 66.6, 61.9, 60.8, 50.84, 29.7, 20.9, 20.8, 20.7, 20.5 ppm.

**Acetylated lactose functionalized dendritic polyglycerol 9.**

Dendritic polyglycerol propargyl ether **6** (3.88 kDa, 21 terminal alkynes), obtained as a butylated hydroxytoluene (BHT) stabilized solution in methanol, was dried down (14 mg, 3 µmol) and reconstituted in 590 µL tetrahydrofuran with lactose azide **4** (50 mg, 67 µmol). Sodium ascorbate (15 mg, 71 µmol) was introduced as a 145 µL aliquot from a 100 mg/mL aqueous solution. Copper (II) sulfate (5 mg, 18.0 µmol) was introduced as a 448 µL aliquot from a 10 mg/mL aqueous solution. The reaction was allowed to stir for 48 h prior to addition of a 600 µL aliquot of 20 mg/mL EDTA solution. After EDTA addition, the reaction was stirred for 1 h. Product **9** was extracted with EtOAc (3 x 3 mL) and dried *in vacuo*. Product was dialyzed against 1000 MWCO tubing in DMSO with progress monitored by TLC (EtOAc, CAM stain) until small molecule spots were no longer observed. The solvent was removed *in vacuo* to afford 43 mg of product **9** (67 % chemical yield) as an oil. $^1$H NMR (500 MHz, $CDCl_3$) δ 7.73 (bs, 1H, triazole), 5.27 (d, J = 3.1 Hz, 1H, H4'), 5.17 (t, J = 9.3 Hz, 1H), 5.08 (dd, J = 10.4, 7.9 Hz, 1H), 4.89 (dd, J = 10.4, 3.4 Hz, 1H), 4.87 (dd, J = 9.5, 7.9 Hz, 1H), 4.55 (d, J = 7.9 Hz, 1H), 4.52 - 4.42 (m, 3H), 4.19 - 4.01 (m, 3H), 3.96 - 3.74 (m, 5H), 3.75 - 3.40 (m, 9H), 3.38 - 3.29 (ap. t, J = 5.1 Hz), 2.12 (s, 3H), 2.09 (s, 3H), 2.03 (s, 3H), 2.02 (s, 6H), 1.99 (s, 3H), 1.94 (s, 3H), 1.23 (bs, 0.6H), 0.81 (bs, 0.20H) ppm. $^{13}$C NMR (126 MHz, $CDCl_3$) δ 170.3, 170.3, 170.1, 170.0, 169.7, 169.6, 169.0, 169.0, 101.1, 100.6, 76.2, 72.8, 72.6, 71.7, 71.0, 70.6, 70.3, 70.1, 69.1, 69.1, 69.0, 66.6, 62.0, 60.8, 50.7, 20.8, 20.8, 20.7, 20.7, 20.6, 20.6. 20.5 ppm.

**Acetylated lactose functionalized dendritic polyglycerol 10.**

Dendritic polyglycerol propargyl ether **7** (7.85 kDa, 33 terminal alkynes), obtained as a butylated hydroxytoluene (BHT) stabilized solution in MeOH, was dried down (10 mg, 1 µmol, 44 µmol terminal alkyne) and reconstituted in 590 µL tetrahydrofuran with lactose azide **4** (50 mg, 66.0 µmol, 1.5 equiv.). Sodium ascorbate (14 mg, 72 µmol, 1.8 equiv.) was introduced as a 142 µL aliquot from a 100 mg/mL aqueous solution. Copper (II) sulfate (4 mg, 20 µmol, 0.5 equiv.) was introduced as a 448 µL aliquot from a 10 mg/mL aqueous solution. The reaction was allowed to stir for 48 h prior to addition of a 600 µL aliquot of 20 mg/mL EDTA solution. After EDTA addition, the reaction was stirred for 1 h. Product was extracted with EtOAc (3 x 3 mL) and dried *in vacuo*. Product **10** was dialyzed against 1000 MWCO tubing in DMSO with progress monitored by TLC (EtOAc, CAM stain) until small molecule spots were no longer observed. The solution was dried *in vacuo* to afford 42 mg of product **10** (70 % chemical yield) as an oil. $^1$H NMR (500 MHz, $CDCl_3$) δ 7.75 (bs, 1H, triazole), 5.35 (d, J = 3.0 Hz, 1H, H4'), 5.13 (t, J = 9.4 Hz,1H), 5.03 (dd, J = 10.2, 8.0 Hz, 1H),

5.04 - 4.94 (m, 1H), 4.93 - 4.83 (m, 1H), 4.77 (bs, 1H), 4.69 - 4.42 (m, 3H), 4.21 - 4.03 (m, 3H), 3.99 - 3.77 (m, 5H), 3.77 - 3.42 (m, 14H), 2.15 (s, 3H), 2.11 (s, 3H), 2.06 (s, 3H), 2.05 (s, 6H), 2.02 (s, 3H), 1.97 (s, 3H), 1.20 (bs, 0.6H), 0.80 (bs, 0.2H) ppm. $^{13}$C NMR (126 MHz, $CDCl_3$) δ 170.3, 170.3, 170.1, 170.1, 169.7, 169.7, 169.6, 169.13, 169.1, 101.0, 100.6, 76.2, 72.8, 72.6, 71.7, 71.6, 71.0, 70.7, 70.4, 70.2, 69.5, 69.1, 66.6, 62.0, 60.8, 20.9, 20.8, 20.8, 20.7, 20.6, 20.6 20.5 ppm.

**Lactoside functionalized dendritic polyglycerol product 11.**

Protected material **8** was obtained as a brown oil (19 mg) and suspended in 1 mL of MeOH. 5 drops of a 25% w/w solution of NaOMe in MeOH was introduced. The reaction was allowed to stir for 30 min, after which 1 mL of water was added and the reaction was allowed to stir overnight. The pH was neutralized by dropwise addition of 1N HCl (pH paper), then the solution was dialyzed overnight (1000 MWCO dialysis tubing) in Millipore water. Solvent was removed *in vacuo* to afford 8 mg of product **11** (30% chemical yield) as a fluffy white solid. $^1$H NMR (600 MHz, $D_2O$) δ 8.12 (bs, 18H, triazole), 4.72 - 4.59 (ap. br. s, 42H, OH), 4.48 (d, J = 7.8, 34H, H1, H1'), 4.12 - 3.44 (m, 570H, $CH_2$, CH; dPG backbone, carbohydrate), 3.35 (t, J = 8.2 Hz, 1H, H2), 1.33 (bs, 2H, $CH_2$; initiator), 0.85 (bs, 3H, $CH_3$ ; initiator) ppm. $^{13}$C NMR (151 MHz, $D_2O$) δ 126.3, 125.6, 103.0, 102.1, 78.4, 75.4, 74.8, 74.4, 72.8, 72.6, 71.0, 69.8, 68.8, 68.6, 61.0, 60.1, 50.0, 38.7 ppm. SEC-HPLC $M_w$ = 14,700 Da, $M_n$ = 7200 Da, PDI = 2.0.

**Lactoside functionalized dendritic polyglycerol product 12.**

Protected material **9** was obtained as a brown oil (22 mg) and suspended in 1 mL methanol. 5 drops of a 25% w/w solution of sodium methoxide in methanol was introduced. The reaction was allowed to stir for 30 min, after which 1 mL water was added and the reaction was allowed to stir overnight. The pH was neutralized by dropwise addition of 1N HCl (pH paper), then the solution was dialyzed overnight (1000 MWCO dialysis tubing) in Millipore water. Solvent was removed *in vacuo* to afford 13 mg of product **12** (34 % chemical yield) as a fluffy white solid. $^1$H NMR (600 MHz, $D_2O$) δ 7.99 (bs, 19H, triazole), 4.53 (bs, 72H, -OH), 4.35 (d, J = 7.8, 43H, H1, H1'), 3.94 - 3.31 (m, 527H, $CH_2$, CH; dPG backbone, carbohydrate), 3.22 (t, J = 8.5 Hz, 1H, H2), 1.21 (bs, 2H, $CH_2$; initiator), 0.71 (bs, 3H, $CH_3$ ; initiator) ppm. $^{13}$C NMR (151 MHz, $D_2O$) δ 144.3, 144.0, 125.4, 102.9, 102.1, 78.4, 75.3, 74.7, 74.3, 72.8, 72.5, 70.9, 70.4, 69.7, 68.7, 68.5, 68.5, 61.0, 60.3, 60.0, 49.9, 38.7 ppm. SEC-HPLC $M_w$ = 16900 Da, $M_n$ = 8500 Da, PDI = 2.0.

**Lactoside functionalized dendritic polyglycerol product 13.**

Protected material **10** was obtained as a brown oil (19 mg) and suspended in 1 mL MeOH. 5 drops of a 25% w/w solution of NaOMe in MeOH was introduced. The reaction was allowed to stir for 30 min, after which 1 mL water was added and the reaction was allowed to stir overnight. The pH was neutralized by dropwise addition of 1N HCl (pH paper), then the solution was dialyzed overnight (1000 MWCO dialysis tubing) in Millipore water. Solvent was removed *in vacuo* to afford 13 mg of product **13** (44 % chemical yield) as a fluffy white solid.1H NMR (600 MHz, $D_2O$) δ 8.04 (bs, 24H, triazole), 4.57 (bs, 60H, OH), 4.35 (d, J = 7.8, 45H, H1, H1'), 3.94 - 3.31 (m, 735H, $CH_2$, CH; dPG backbone, carbohydrate), 3.22 (t, J = 8.5 Hz, 26H, H2), 1.21 (bs, 2H, $CH_2$ ; initiator), 0.71 (bs, 3H, $CH_3$ ; initiator) ppm. $^{13}$C NMR (151 MHz, $D_2O$) δ 103.0, 102.1, 78.4, 75.4, 74.8, 74.4, 72.8, 72.6, 71.0, 69.8, 69.7, 68.8, 68.6, 61.0, 60.1, 60.0, 50.0, 38.7 ppm. SEC-HPLC $M_w$ = 35700 Da, $M_n$ = 17300 Da, PDI = 2.1.

**Heterogeneously functionalized dendritic polyglycerol 14a.**

Dendritic polyglycerol propargyl ether **7** (7.85 kDa, 44% functionalization, 33 terminal alkynes), obtained as a butylated hydroxytoluene stabilized solution in methanol, was dried down (14 mg, 2 µmol, 60 µmol terminal alkyne) and reconstituted in 590 µL tetrahydrofuran with lactose azide **4** (51 mg, 68 µmol) and 2-(2-azidoethoxy)ethanol **3** (3 mg, 20 µmol). Sodium ascorbate (18 mg, 91 µmol) was introduced as a 180 µL aliquot from a 100 mg/mL aqueous solution. Copper (II) sulfate (7 mg, 30 µmol) was introduced as a 68 µL aliquot from a 100 mg/mL aqueous solution. The reaction was allowed to stir for 24 h prior to addition of a 600 µL aliquot of 20 mg/mL EDTA solution. After addition of EDTA, the reaction was allowed to stir for 1 h. The product was extracted with EtOAc (3 x 3 mL) and solvent was removed *in vacuo*. Product was dialyzed against 1000 MWCO tubing in DMSO with progress monitored by TLC (EtOAc, CAM stain) until small molecule spots were no longer observed. The solvent was removed *in vacuo* to afford 34 mg of **14** (47 % chemical yield) as a yellow brown oil. $^1$H NMR (500 MHz, $CDCl_3$) δ 7.74 (bs, 33H, triazole), 5.32 (ap. s, 36H), 5.16 (t, J = 9.4 Hz, 36H), 5.10 - 5.03 (m, 36H), 4.95 (ap. d, J = 10.3 Hz, 36H), 4.85 (t, J = 6.5 Hz, 36H), 4.74 (bs, 36H), 4.66 - 4.38 (m, 200H), 4.15 - 4.03 (m, 113H), 4.00 - 3.76 (m, 232H), 3.76 - 3.29 (m, 565H), 2.15 (s, 112H), 2.08 (s, 100H), 2.05-2.01 (m, 343H), 1.99 (s, 193H), 1.94 (s, 127H), 1.20 (bs, 7H), 0.80 (bs, 3H) ppm. $^{13}$C NMR (126 MHz, $CDCl_3$) δ 170.3, 170.3, 170.1, 170.1, 169.7, 169.7, 169.6, 169.13, 169.1, 101.0, 100.6, 76.2, 72.8, 72.6, 71.7, 71.6, 71.0, 70.7, 70.4, 70.2, 69.5, 69.1, 66.6, 62.0, 60.8, 20.9, 20.8, 20.8, 20.7, 20.6, 20.6 20.5 ppm.

**Heterogeneously functionalized dendritic polyglycerol 15a and 16a.**

Dendritic polyglycerol propargyl ether **7** (7.85 kDa, 44% functionalization, 33 terminal alkynes), obtained as a butylated hydroxytoluene stabilized solution in MeOH, was dried down (22 mg, 2.8 µmol, 93 µmol terminal alkyne) and reconstituted in 590 µL tetrahydrofuran with lactose azide **4** (54 mg, 72 µmol) and 2-(2-azidoethoxy)ethanol **3** (9 mg, 70 µmol). Sodium ascorbate (28 mg, 144 µmol) was introduced as a 285 µL aliquot from a 100 mg/mL aqueous solution. Copper (II) sulfate (11 mg, 27 µmol) was introduced as a 107 µL aliquot from a 100 mg/mL aqueous solution. The reaction was allowed to stir for 24 h prior to addition of a 600 µL aliquot of 20 mg/mL EDTA solution. After addition of EDTA, the reaction was allowed to stir for 1 h. Product **15a** was extracted with EtOAc (3 x 3 mL) and dialyzed against 1000 MWCO tubing in DMSO with progress monitored by TLC (EtOAc, CAM stain) until small molecule spots were no longer observed. The solvent was removed *in vacuo* to afford 16 mg of 17 (19 % chemical yield) as a yellow brown oil. $^1$H NMR

(500 MHz, $CDCl_3$) δ 7.74 (bs, 33H, triazole), 5.31 (d, J = 3.4 Hz, 49H), 5.16 (t, J = 9.4 Hz, 37H), 5.10 - 5.03 (m, 54H), 4.95 (ap. d, J = 10.3 Hz, 50H), 4.85 (t, J = 6.5 Hz, 51H), 4.66 - 4.38 (m, 215H), 4.15 - 4.03 (m, 183H), 4.00 - 3.76 (m, 316H), 3.76 - 3.29 (m, 644H), 2.12 (s, 153H), 2.09 (s, 150H), 2.04 - 1.95 (m, 624H), 1.93 (s, 181H), 1.94 (s, 127H), 1.20 (bs, 138H), 0.80 (bs, 24H) ppm. $^{13}C$ NMR (126 MHz, $D_2O$) δ 170.3, 170.1, 170.0, 170.0, 169.7, 169.6, 169.1, 169.0, 101.0, 100.6, 76.2, 72.8, 72.6, 71.7, 70.6, 70.3, 70.1, 69.1, 69.0, 69.0, 66.6, 60.8, 50.7, 41.0, 29.7, 20.9, 20.8, 20.8, 20.7, 20.6, 20.5 ppm.

Product **16a**, retained in the water layer during extraction, was dialyzed against 1000 MWCO tubing in Millipore water with progress monitored by TLC (EtOAc, CAM stain) until small molecule spots were no longer observed. The solvent was removed *in vacuo* to afford 15 mg of **16a** (18 % chemical yield) as a green oil. $^1H$ NMR (500 MHz, $D_2O$) δ 8.20 (bs, 33H, triazole), 5.46 (ap. s, 7H), 5.20 (bs, 21H), 5.04 (bs, 22H), 4.23 (bs, 47H), 4.00 (bs, 262H), 3.91 (bs, 93H), 3.85 - 3.43 (m, 1576H), 2.24 - 2.03 (m, 172H), 1.34 (bs, 5H), 0.86 (bs, 2H) ppm. $^{13}C$ NMR (126 MHz, $D_2O$) δ 72.1, 71.7, 68.7, 48.9 ppm.

**Heterogeneously functionalized dendritic polyglycerol 17a.**

Dendritic polyglycerol propargyl ether **7** (6.99 kDa, 44% functionalization, 33 terminal alkynes), obtained as a butylated hydroxytoluene stabilized solution in methanol, was dried down (22 mg, 2.8 µmol, 91 µmol terminal alkyne) and reconstituted in 590 µL tetrahydrofuran with lactose azide **4** (28 mg, 37 µmol) and 2-(2-azidoethoxy)ethanol **3** (14 mg, 110 µmol). Sodium ascorbate (29 mg, 147 µmol) was introduced as a 292 µL aliquot from a 100 mg/mL aqueous solution. Copper (II) sulfate (11 mg, 27 µmol) was introduced as a 110 µL aliquot from a 100 mg/mL aqueous solution. The reaction was allowed to stir for 24 h prior to addition of a 600 µL aliquot of 20 mg/mL EDTA solution. After addition of EDTA, the reaction was allowed to stir for 1 h. Small molecules were extracted with EtOAc (3 x 3 mL). Product **17**, retained in the water layer during extraction, was dialyzed against 1000 MWCO tubing in Millipore water with progress monitored by TLC (EtOAc, CAM stain) until small molecule spots were no longer observed. The solvent was removed *in vacuo* to afford 15 mg of **17** (23 % chemical yield) as a green oil. $^1H$ NMR (500 MHz, $D_2O$) δ 8.23 (bs, 33H, triazole), 5.45 (ap. s, 5H), 5.19 (bs, 11H), 5.04 (bs, 12H), 4.67 (bs, 134H), 4.23 (bs, 19H), 4.00 (bs, 208H), 3.85 - 3.43 (m, 873H), 2.23 (s, 7H), 2.15- 2.03 (m, 40H), 1.34 (bs, 10H), 0.86 (bs, 5H) ppm. $^{13}C$ NMR (126 MHz, $D_2O$) δ172.8, 72.2, 71.7, 70.4, 69.2, 68.7, 60.3, 50.2, 48.9 ppm.

**Lactoside functionalized dendritic polyglycerol product 14.**

Protected material **14** was obtained as a brown oil (17 mg) and suspended in 1 mL methanol. 5 drops of a 25% w/w solution of NaOMe in MeOH was introduced. The reaction was allowed to stir for 30 min, after which 1 mL water was added and the reaction was allowed to stir overnight. The pH was neutralized by dropwise addition of 1N HCl (pH paper), then the solution was dialyzed overnight (1000 MWCO dialysis tubing) in Millipore water. Solvent was removed *in vacuo* to afford 7 mg of product **18** (30 % chemical yield) as a fluffy white solid. $^1H$ NMR (600 MHz, $D_2O$) δ 8.11 (bs, 33H, triazole), 4.61 (bs, 106H, OH), 4.48 (d, J = 7.8, 54H, H1, H1'), 4.12 - 3.44 (m, 976H, $CH_2$, CH; dPG backbone, carbohydrate), 3.35 (t, J = 8.2 Hz, 36H, H2), 1.33 (bs, 2H, $CH_2$; initiator), 0.86 (bs, 3H, $CH_3$; initiator) ppm. $^{13}C$ NMR (151 MHz, $D_2O$) δ 125.4, 103.0, 102.1, 78.4, 75.4, 74.7, 74.4, 72.8, 72.5, 72.1, 71.7, 71.0, 70.4, 69.8, 68.8, 68.6, 61.0, 60.7, 60.3, 60.1, 49.9 ppm. SEC-HPLC $M_w$ = 46,800 Da, $M_n$ = 20,600 Da, PDI = 2.3.

**Lactoside functionalized dendritic polyglycerol product 15.**

Protected material **15** was obtained as a brown oil (16 mg) and suspended in 1 mL methanol. 5 drops of a 25% w/w solution of NaOMe in MeOH was introduced. The reaction was allowed to stir for 30 min, after which 1 mL water was added and the reaction was allowed to stir overnight. The pH was neutralized by dropwise addition of 1N HCl (pH paper), then the solution was dialyzed overnight (1000 MWCO dialysis tubing) in Millipore water. Solvent was removed in vacuo to afford 8 mg of product **15** (41 % chemical yield) as a fluffy white solid. $^1H$ NMR (600 MHz, $D_2O$) δ 8.07 (bs, 33H, triazole), 4.61 (bs, 100H, OH), 4.48 (d, J = 7.8, 40H, H1, H1'), 4.12 - 3.44 (m, 853H, $CH_2$, CH; dPG backbone, carbohydrate), 3.35 (t, J = 8.2 Hz, 29H, H2), 1.33 (bs, 2H, $CH_2$; initiator), 0.86 (bs, 3H, $CH_3$; initiator) ppm. $^{13}C$ NMR (151 MHz, $D_2O$) δ 144.3, 143.9, 125.4, 102.9, 102.1, 78.4, 75.3, 74.7, 74.3, 72.8, 72.5, 72.1, 71.7, 70.9, 69.7, 68.7, 68.5, 63.4, 62.2, 61.0, 60.3, 60.0, 50.0, 49.9 ppm. SEC-HPLC $M_w$ = 62000 Da, $M_n$ = 25700 Da, PDI = 2.4.

**Lactoside functionalized dendritic polyglycerol product 16.**

Protected material **16** was obtained as a brown oil (15 mg) and suspended in 1 mL methanol. 5 drops of a 25% w/w solution of NaOMe in MeOH was introduced. The reaction was allowed to stir for 30 min, after which 1 mL water was added and the reaction was allowed to stir overnight. The pH was neutralized by dropwise addition of 1N HCl (pH paper), then the solution was dialyzed overnight (1000 MWCO dialysis tubing) in Millipore water. The solvent was removed *in vacuo* to afford 9 mg of product **20** (55 % chemical yield) as a clear, light green oil. $^1H$ NMR (600 MHz, $D_2O$) δ 8.09 (bs, 33H, triazole), 4.63 (bs, 98H, -OH), 4.48 (d, J = 7.8, 8H, H1, H1'), 4.12 - 3.30 (m, 928H, -CH2 , -CH; dPG backbone, carbohydrate), 1.33 (bs, 2H, $CH_2$; initiator), 0.86 (bs, 3H, $CH_3$ ; initiator) ppm. $^{13}C$ NMR (151 MHz, $D_2O$) δ 215.4, 144.3, 125.4, 102.9, 78.4, 78.0, 77.5, 77.3, 75.3, 74.7, 74.3, 72.8, 72.5, 72.1, 71.7, 70.9, 70.8, 70.4, 69.8, 69.1, 68.7, 68.5, 63.4, 62.6, 62.2, 61.0, 60.7, 60.3, 60.0, 50.0, 30.2 ppm. SEC-HPLC $M_w$ = 33500 Da, $M_n$ = 13300 Da, PDI = 2.5.

**Lactoside functionalized dendritic polyglycerol product 17.**

Protected material **17** was obtained as a brown oil (15 mg) and suspended in 1 mL methanol. 5 drops of a 25% w/w solution of NaOMe in MeOH was introduced. The reaction was allowed to stir for 30 min, after which 1 mL water was added and the reaction was allowed to stir overnight. The pH was neutralized by dropwise addition of 1N HCl (pH paper), then the solution was dialyzed overnight (1000 MWCO dialysis tubing) in Millipore water. The solvent was removed *in vacuo* to afford 10 mg of product **21** (65 % chemical yield) as a clear, light green oil. $^1H$ NMR (600 MHz, $D_2O$) δ 8.09 (bs, 33H, triazole), 4.62 (bs,

106H, OH), 4.44 (d, J = 7.8, 2H, H1, H1'), 4.12 - 3.30 (m, 765H, $CH_2$, CH; dPG backbone, carbohydrate), 1.33 (bs, 2H, $CH_2$; initiator), 0.86 (bs, 3H, $CH_3$; initiator) ppm. $^{13}C$ NMR (151 MHz, $D_2O$) δ 144.3, 143.9, 125.4, 78.0, 72.1, 71.7, 70.8, 70.4, 69.1, 68.7, 63.4, 62.6, 62.2, 60.7, 60.3, 50.0, 30.2 ppm. SEC-HPLC $M_w$ =36700 Da, $M_n$ = 13700 Da, PDI = 2.7.

**Dynamic Light Scattering.**

Hydrodynamic radii ($R_h$) of individual analytes and aggregates were measured on a Wyatt Möbius DLS instrument in PBS with a 45 µL quartz cuvette. Analyte solutions were filtered through 0.02 µm filters (Whatman Anotop 25) until single species were observed. Individual analyte solutions were measured before and after aggregation experiments to ensure observed aggregation was not the result of self-aggregation.

**Determination of $R_h$ for LdPG/galectin-3 aggregates.**

LdPGs were dissolved in PBS to 50 µM and allowed to equilibrate overnight before filtering. Galectin-3, LdPG and PBS solutions were filtered until single representative species were observed by DLS. Galectin-3 solution was diluted with PBS to produce a final protein concentration of 22 µM upon addition of the LdPG solution. LdPG solution was introduced to achieve protein/polymer ratios of 2:1, 6:1 or 150:1. Once mixed, each solution was briefly vortexed, then allowed to incubate at 21 °C for 1 h. This aggregate solution was vortexed for 5 s, allowed to rest for 1 min, then analyzed by DLS. DLS source attenuation was allowed for the first scan of a given sample, then auto-attenuation was turned off. Trials interrupted by attenuation were discarded. Three solutions were made up for each concentration ratio and for each LdPG and allowed to incubate individually. Reported data, based on triplicate measurement for each solution, were determined using a regularization fit for an inclusive range of the autocorrelation function.

**Determination of $R_h$ for LdPG/galectin-3 CRD aggregates.**

LdPG **13** was dissolved in PBS to 50 µM and allowed to equilibrate overnight before filtering. Galectin-3 CRD, LdPG and PBS solutions were filtered until single representative species were observed by DLS. Galectin-3 CRD solution was diluted with PBS to produce a final protein concentration of 20 µM upon addition of the LdPG solution. LdPG solution was introduced to achieve protein/polymer ratios of 2:1, 6:1 or 150:1. Once mixed, each solution was briefly vortexed, then allowed to incubate at 21 °C for 1 h in order to form maximally sized aggregates. This aggregate solution was vortexed for 5 s, allowed to rest for 1 min, then analyzed by DLS. DLS source attenuation was allowed for the first scan of a given sample, then auto-attenuation was turned off. Trials interrupted by attenuation were discarded. Three solutions were made up for each concentration ratio and allowed to incubate individually. Reported data, based on triplicate measurement for each solution, were determined using a regularization fit for an inclusive range of the autocorrelation function.

**Determination of $R_h$ for dPG/galectin-3 aggregate.**

10 kDa dPG was dissolved in PBS to 25 µM. Galectin-3, dPG and PBS solutions were filtered until single representative species were observed by DLS. Galectin-3 solution was diluted with PBS to produce a final protein concentration of 10 µM upon addition of the dPG solution. dPG solution was introduced to achieve protein/polymer ratios of 2:1, 6:1 or 150:1. Once mixed, each solution was briefly vortexed, then allowed to incubate at 21 °C for 1 h in order to form maximally sized aggregates. This aggregate solution was vortexed for 5 s, allowed to rest for 1 min, then analyzed by DLS. DLS source attenuation was allowed for the first scan of a given sample, then auto-attenuation was turned off. Trials interrupted by attenuation were discarded. Three solutions were made up for each concentration ratio and for each LdPG and allowed to incubate individually. Reported data, based on triplicate measurement for each solution, were determined using a regularization fit for an inclusive range of the autocorrelation function.

**Determination of $R_h$ for carbohydrate/galectin-3 aggregates.**

Lactose and mannose were dissolved in PBS to 50 µM. Galectin-3, carbohydrate and PBS solutions were filtered until single representative species were observed by DLS. Galectin-3 solution was diluted with PBS to produce a final protein concentration of 22 µM upon addition of the carbohydrate solution. Carbohydrate solution was introduced to achieve protein/polymer ratios of 2:1 and 6:1. Once mixed, each solution was briefly vortexed, then allowed to incubate at 21 °C for 1 h in order to form maximally sized aggregates. This aggregate solution was vortexed for 5 s, allowed to rest for 1 min, then analyzed by DLS. DLS source attenuation was allowed for the first scan of a given sample, then auto-attenuation was turned off. Trials interrupted by attenuation were discarded. Three solutions were made up for each concentration ratio and for each LdPG and allowed to incubate individually. Reported data, based on triplicate measurement for each solution, were determined using a regularization fit for an inclusive range of the autocorrelation function.

## Results

**Synthesis of lactose functionalized dPGs.**

For formation of lactose functionalized dPGs, a peracetylated lactoside attached to a short linker at the anomeric position that has a terminal azido group was needed. This requisite compound is shown in Scheme 1 as compound **4**, the synthesis of which starts with peracetylation of lactose. We modified our previously published protocol[33] by using only 1.55 equiv. of acetic anhydride per alcohol in a solvolysis reaction with a catalytic amount of indium triflate (0.1 mol %) to afford peracetylated lactoside (70% yield). Selective deacetylation at the anomeric position afforded **1** (86% yield). Installation of the trichloroacetimidate at the anomeric position was achieved with diastereoselectivity to afford the thermodynamically favored *α* anomer **2** in 69% yield by using 1,8-diazabicyclo[5.4.0]undec-7-ene (DBU). Azidoethoxyethanol **3**

was added to trichloroacetimidate **2** to afford the key lactoside derivative **4** in 62% yield.

Starting material dPGs that led to the successful synthesis of lactose functionalized dendritic polyglycerols were purchased from Nanopartica GmbH as a 2.5, 5, and 10 kDa dPG research kit (Berlin, Germany).[34] The polymers are shown schematically in Fig. 1.

Functionalization of these alcohol terminal dPGs to form **11-13** is shown in Scheme 2. Formation of propargyl ether intermediates **5**-**7** was accomplished via a Williamson ether synthesis. Quantification of the percent functionalization of the dPGs was determined by $^1$H NMR; the integrations of the characteristic dPG resonances and the signals for the propargyl endgroups were compared. The addition of each glycidol monomer to the dPG structure adds 5 protons. Therefore, integration ratios comparing the dPG backbone signal (3.98 - 3.36 ppm in $CD_3OD$) to the 3 signals corresponding to propargyl protons and the acetylenic proton (4.35 (bs), 4.12 (bs), and 2.90 (bs), respectively), were used to determine the degree of functionalization of the polymer.

Addition of lactosides was achieved through copper (I) mediated click chemistry,[32] coupling the azide of **4** with the alkyne endgroups of **5-7** to afford **8-10** with 1,4-triazole linkages. Optimization of the Huisgen reaction included screening classical click chemistry conditions[35] and highly pertinent conditions previously reported by the Haag group.[32] Quantitative reaction of the terminal alkynes of **5-7** was realized using $CuSO_4$ with sodium ascorbate in 1:1 THF/$H_2O$, resulting in products **8-10**. Formation of the final products **11-13** was achieved through deprotection using Zemplen conditions.

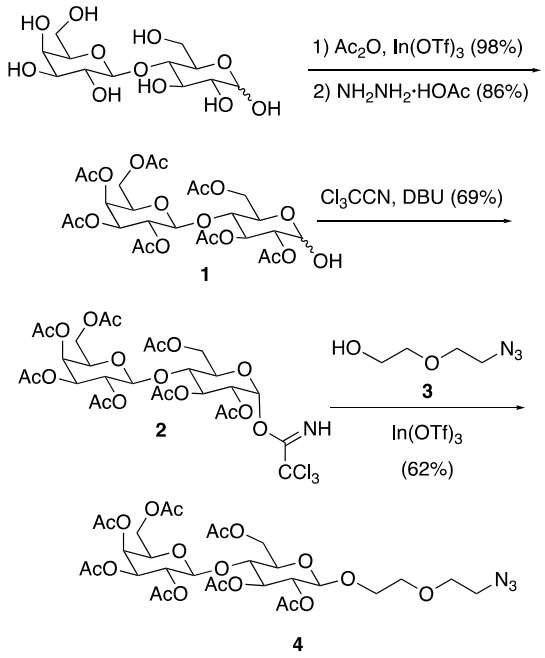


**Scheme 1** Synthesis of lactoside derivatives for functionalization of dPGs.

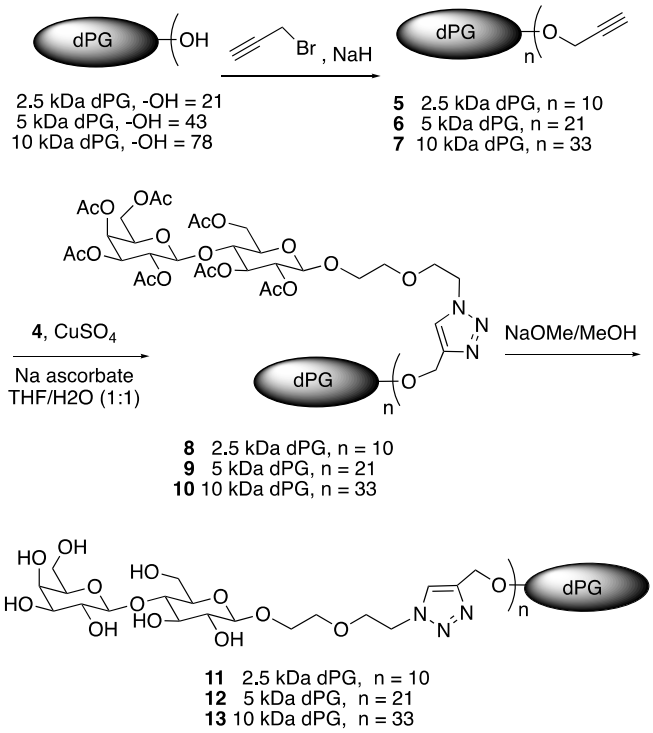


**Scheme 2** Synthesis of lactoside functionalized dPGs.

Characterization of glycopolymers **11-13** was carried out using NMR and size exclusion chromatography (SEC-HPLC) and is tabulated in Table 1. The specifics of the SEC-HPLC analysis can be found in the electronic supplementary information. Key features of these NMRs include the broadened peaks characteristic of polymeric materials. Specifically, the doublet at 4.5 ppm is characteristic of the axial anomeric protons (H-1, H-1') for the glucoside and galactoside moieties, and the broad downfield singlet at 8.1 ppm is characteristic of a triazole proton. For LdPGs **11-13**, the ratio of integrations for these peaks is 2:1 anomeric protons per triazole.

**Table 1** Characterization information for glycopolymers **11-13**.

| Cmpd | % funct. (# lactose) | Radius (nm) | $M_W$[a] (kDa) | $M_N$[b] (kDa) | PDI[c] |
|---|---|---|---|---|---|
| **11** | 48 (10) | 5.9 ± 0.4 | 14.7 | 7.2 | 2.0 |
| **12** | 48 (21) | 4.2 ± 0.3 | 16.9 | 8.5 | 2.0 |
| **13** | 44 (33) | 3.7 ± 0.3 | 35.7 | 17.3 | 2.1 |

[a]$M_W$ = weight average molecular weight. [b]$M_N$ = number average molecular weight. [c]PDI = polydispersity index.

In order to better understand the relationship between percent functionalization and multivalent binding, a series of heterogeneously functionalized 10 kDa LdPGs were synthesized with fewer lactosides than were present on **13**, as shown in Scheme 3. Polymers **14**-**17** were produced from propargylated dPG **7**. 2-(2-azidoethoxy)ethanol **3** and the lactose azide **4** were added concurrently via a one-pot reaction. Presumably, the difference in kinetics (the smaller azide **3** reacting more rapidly than **4**) led to a measurable difference in the polydispersity of the heterogeneously functionalized LdPG final products

**14**-**17** (Table 2) when compared to the polydispersity of the homogeneously lactose functionalized products **11**-**13**. Stepwise synthesis of **14**-**17** was briefly explored, but complications in purification and characterization stalled progress and led ultimately to the development of the concerted procedure.

**Table 2** Characterization information for glycopolymers **14-17**.

| Cmpd | % funct. (# sugars) | Radius (nm) | $M_W$[a] (kDa) | $M_N$[b] (kDa) | PDI[c] |
|---|---|---|---|---|---|
| **14** | 36 (27) | 2.6 ± 0.1 | 46.8 | 20.6 | 2.3 |
| **15** | 26 (20) | 2.8 ± 0.4 | 62.0 | 25.7 | 2.4 |
| **16** | 5 (14) | 2.9 ± 0.4 | 33.5 | 13.3 | 2. 5 |
| **17** | 3 (1) | 3.5 ± 0.3 | 36.7 | 13.7 | 2.7 |

[a]$M_W$ = weight average molecular weight. [b]$M_N$ = number average molecular weight. [c]PDI = polydispersity index.

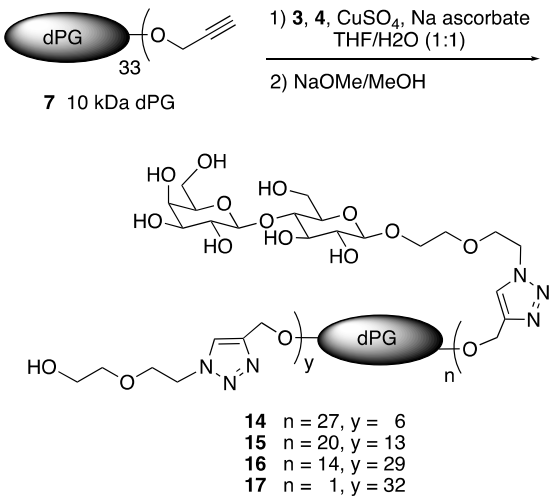


**Scheme 3** Synthesis of heterogeneously functionalized LdPGs bearing lactosides and hydroxyl groups.

Increasing the degree of functionalization with of 2-(2-ethoxy)ethanol endgroups caused a marked increase in the aqueous solubility of the peracetylated lactose functionalized dPGs relative to LdPG peracetylated intermediates with a higher percentage incorporation of protected lactoside **4**. Attempts to remove copper by extraction in EDTA (20 mg/mL) proved problematic for polymers with a higher number of 2-(2-ethoxy)ethanol endgroups because they were retained in the aqueous layer. In fact, products **16** and **17** resulted from splitting the organic and aqueous layers of work-up for a single reaction.

For heterogeneously functionalized LdPGs **14**-**17**, the ratio of the integrations of resonances from the anomeric protons (4.5 ppm) and the triazole protons (8.1 ppm) was used to determine the percent functionalization of the LdPGs (Table 2).

For size characterization of **11**-**17**, and for PDI calculations, SEC-HPLC was performed. Lactose functionalized PAMAM dendrimers, whose mass characteristics were readily observed by MALDI-TOF MS,[33] were selected as calibration standards. Using SEC-HPLC, the molar mass averages ($M_W$ and $M_N$) and PDI were determined (Tables 1 and 2). Products **11**-**13** exhibited the moderate polydispersity (PDI ~2) that is characteristic of dendritic polyglycerols, whereas the polydispersity was increased to varying degrees in the heterogeneously functionalized products **14**-**17**. Presumably, the increased polydispersity of **14**-**17** arises due to reactivity differences between **3** and **4**.

**Aggregation studies using galectin-3 with lactose functionalized dPGs.**

DLS measurements were taken for lactoside functionalized dPGs **11**-**17**. Lactoside functionalized dendritic polyglycerol polymers **11**-**13**, which all have the same percent functionalization but vary in terms of the size of the dPG framework, exhibited a notable trend; the hydrodynamic radius ($R_H$) is inversely proportional to molecular weight (Table 1). A heavier polymer occupies less space. Evidently, intramolecular hydrogen bonding prevails when more glycosidic alcohols and internal alcohols are available to interact, condensing the structure. Furthermore, the entropic impact of increased degrees of freedom in a larger polymer may be relieved when the polymer folds in upon itself. Examples of the phenomenon have previously been reported.[36]

For the aggregation studies reported here, a small excess and a significant excess of galectin-3 (2:1 and 6:1, respectively) were used to observe the differences between systems that bind stoichiometrically versus those that would have the nucleating polymer more surrounded by galectin-3. A much higher excess of galectin-3 (150:1) was also implemented to observe the effects of saturation on galectin-3 binding to the polymers. Polymer concentrations for the experiments were chosen such that, even at the highest concentrations of LdPGs used, the solutions were below the critical aggregation concentration (CAC) of the LdPGs. Thus, any aggregation that was observed during the reported DLS experiments would not be due to self-aggregation of either the LdPGs or the galectin-3 (which was also well below its CAC). It is important to note that no self-aggregation was observed in the unmixed analyte solutions during the allotted aggregation time.

The concentration of galectin-3 that was used in the experiments reported here was chosen based on the concentration of lactose functionalized dPG used in the 150:1 experiments. To facilitate data comparison across the 31 experimental conditions reported herein, which were run under triplicate conditions, the galectin-3 concentration in the 93 runs reported herein was kept constant. When galectin-3 was used at higher concentrations in test experiments (32 μM rather than 22 μM) or at a lower concentration as reported below for studies with the unfunctionalized dPG (10 μM), the same radii of aggregates were observed.

Galectin-3 aggregation nucleated by LdPGs demonstrated that small glycopolymers **11**-**14** (2.6 nm < $R_H$ < 5.9 nm) and galectin-3 (6.4 ± 0.4 nm) come together to form reasonably large aggregates. These aggregates have size characteristics that are highly reproducible and surprisingly homogenous, as evidenced by the relatively small error bars in Fig. 2.

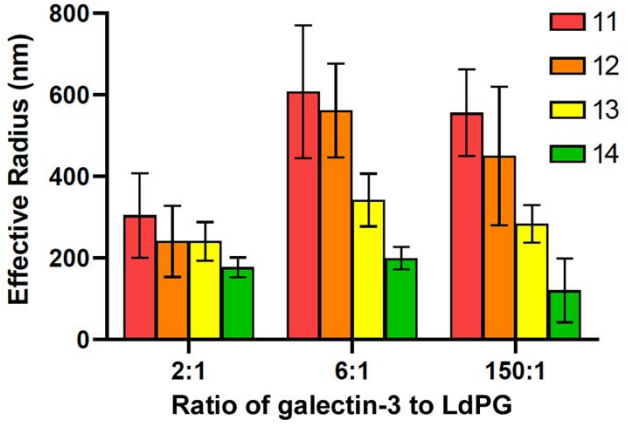


**Fig. 2** DLS results showing that the size of the galectin-3/LdPG aggregate decreases as the hydrodynamic radius of the LdPG decreases for 6:1 and 150:1 ratios of galectin-3/LdPG with **11**-**14**.

Although all aggregate sizes were approximately the same for 2:1 ratios of galectin-3/LdPG using **11-14**, the effective radii observed for galectin-3/LdPG aggregates with 6:1 and 150:1 ratios of galectin-3:LdPG decreased as the hydrodynamic radius of the nucleating polymer decreased (in Fig. 2, compare aggregates formed using **11** (red bars) and using **14** (green bars), for example). Results for **14** with galectin-3 are included in Fig. 2 because the hydrodynamic radius of **14** fits the trend of reduced $R_H$ with increased molecular weight. The trend for aggregate size when galecin-3 and LdPG are mixed is also conserved for **14**.

Galectin-3 does not appear to self-aggregate without a motive force such as a nucleating glycopolymer or high concentration. Following long term storage (6 weeks at 4 °C) in PBS at 15 μM, the hydrodynamic radius for galectin-3 was maintained at 6.4 ± 0.4 nm (Fig. S47 in the electronic supporting information). Without the *N*-terminal tail domain, the galectin-3 CRD exhibits a smaller hydrodynamic radius of 2.9 ± 0.2 nm (Fig. S47) and also does not demonstrate any self-aggregating processes over several weeks in PBS.

Relative to the LdPG induced nucleation of galectin-3, the effective radii observed for galectin-3 with monomeric carbohydrates were observable but very small, as shown in Fig. 3. Aggregates in the size range expected for formation of dimers or trimers seem to be formed, most likely induced by nonspecific binding of galectin-3 lectins to the carbohydrates. Galectin-3/lactoside measurements were 20 ± 10 and 15 ± 4 nm for 2:1 and 6:1 galectin-3/lactoside ratios, respectively. The effective radii observed for galectin-3 with monomeric mannose were comparable to those with monomeric lactose. Since mannose does not bind in the galactoside binding pocket of galectin-3, the comparable (slight) aggregation observed for monomeric lactose and mannose supports the suggestion that a small amount of nonspecific aggregation of galectin-3 can occur in the presence of monosaccharides. Mannose does not bind in the galactoside binding cleft of the CRD. Since carbohydrates have been used to mimic intracellular molecular crowding in other systems,[37] a small amount of protein aggregation in the presence of monosaccharides is not unexpected. The effective radii observed for a truncated galectin-3 CRD with LdPG **13** were 4 ± 2, 8 ± 1, and 2.6 ± 0.2 nm for 2:1, 6:1, and 150:1 galectin-3 CRD/glycopolymer ratios, respectively (Fig. 3). These values are too small to indicate any aggregation, revealing that the *N*-terminal domain is required for galectin-3 aggregation to occur. Finally, DLS experiments using the truncated CRD with monomeric lactose and mannose do not lead to aggregation, indicating that the small aggregates formed by monomeric carbohydrates with galectin-3 involve aggregation processes with the *N*-terminal domain rather than specific protein-carbohydrate binding interactions.

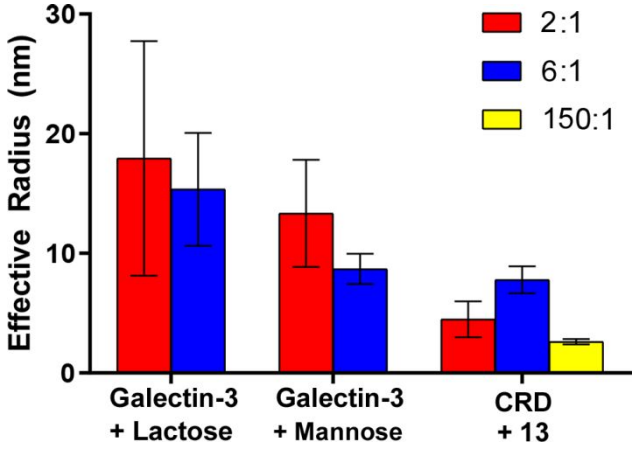


**Fig. 3** DLS results for monomeric carbohydrates with galectin-3 and for LdPG **13** with the CRD of galectin-3.

When employing dendritic polyglycerols with minimal or no lactose functionalization (LdPGs **15**-**17** and the parent 10 kDa unfunctionalized dPG), large and highly irregular aggregates were observed (Fig. 4). This is in contrast to the 10 kDa LdPGs **13** and **14**, which have 44% and 36% lactoside functionalization, respectively. Both **13** and **14** nucleate formation of aggregates with narrower size distributions, as shown in Fig. 2, strongly suggesting that specific galectin-3 receptor/galactose carbohydrate binding interactions in the CRD binding pocket govern aggregate formation for LdPGs with at least 35% functionalization.

The effective radii observed for aggregates nucleated by partially lactose functionalized LdPGs **15**, **16**, and **17** are shown in Fig 4. The effective radii observed for aggregates nucleated by a 10 kDa dPG, featuring stock terminal alcohols but entirely without lactoside functionalization, were comparable to the results with **15-17** (Fig. 4). Thus, aggregate formation for LdPGs with less than 35% lactose incorporation is indistinguishable from the nonspecific association that occurs without utilizing the galactose/galectin-3 binding interaction.

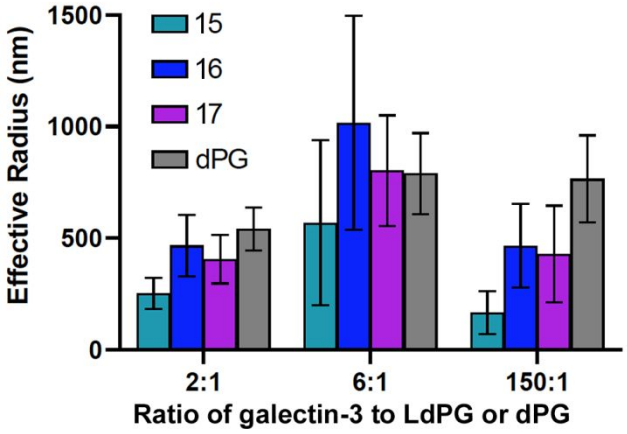


**Fig. 4** DLS results for galectin-3/dPG aggregation using 10 kDa dPGs functionalized with decreasing amounts of lactosides, and 10 kDa dPG without any lactose functionalization.

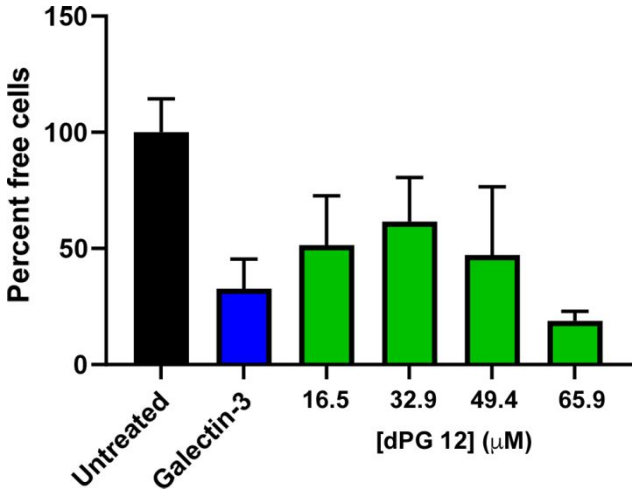


**Fig. 5** Effects of increasing concentrations of LdPG **12** on galectin-3 induced cancer cellular aggregation using DU-145 prostate cancer cells.

**Cancer cellular aggregation studies using galectin-3 and lactose functionalized dPGs.**

Cancer cellular aggregation studies are the *in vitro* model for tumor formation. The cellular aggregation assay with compound **12**, the 5 kDa LdPG functionalized with an average of 21 lactosides, effectively demonstrates the interplay between the importance of the hydrodynamic radius of the glycopolymer and the degree of carbohydrate functionalization (Fig. 5). Previous studies using lactose functionalized dendrimers showed that small dendrimers bearing a comparable number of lactosides inhibited galectin-3 mediated cellular aggregation (lactose functionalized [G2] and [G3]-PAMAMs). Dendrimers with a comparable hydrodynamic radius, however, enhanced cellular aggregation (lactose functionalized [G6]-PAMAMs).[26] LdPG **12** with on average 21 lactosides and a hydrodynamic radius of 4.2 $\pm$ 0.3 nm is therefore an interesting molecule to study because, although the effects are small, the enhancement of cancer cellular aggregation at high concentrations of **12** trends with the enhancement induced by similarly sized glycodendrimers (lactose functionalized [G6]-PAMAM). The inhibition of aggregation at lower concentrations, on the other hand, trends with glycodendrimers bearing a similar degree of lactoside functionalization (lactose functionalized [G2] and [G3]-PAMAMs, Fig. 5). Thus, the results reported in Fig. 5 for **12** indicate that both the hydrodynamic radius and the degree of lactose functionalization strongly influence cancer cellular aggregation, with the different effects becoming predominant at different concentrations of **12**.

## Discussion

A series of lactose functionalized dendritic polyglycerols **11**-**17** was produced via a quantitative copper (I) mediated click chemistry approach, coupling lactoside endgroups to dPGs via triazole linkages as described above and summarized in Tables 1 and 2.

The PDI of the lactose functionalized 2.5 kDa dPG **11** is unchanged relative to the PDI of the unfunctionalized dPG (2.03 for **11** and 1.99 for the dPG starting material). The PDIs for the 5 kDa and the 10 kDa dPGs increase upon functionalization from 1.6 and 1.4 to 2.0 and 2.1 (Table 1). Evidently, as the dPGs increase in molecular weight and in number of terminal alcohols, the complexity of the material increases concurrently. Because of the increased complexity of the larger dPGs relative to the 2.5 kDa dPG, the sample heterogeneity increases for **12** and **13** upon functionalization. However, the PDIs of lactose functionalized dendrimers **11**-**13** remain comparable to values for previously reported dPGs.[34] Even when azides **3** and **4** are concurrently introduced to form **14**-**17**, the PDIs remain reasonably low (Table 2).

When employing LdPGs **11**-**13** with the highest degree of lactose functionalization that was studied (44-48%), discrete and reproducible aggregates were formed as shown in Fig. 2. Critically, the size of the protein/polymer aggregate correlated with the hydrodynamic radius of the polymer; as the radius of the LdPG increased, the size of the aggregate also increased for 6:1 and 150:1 galectin-3/LdPG ratios even though the molecular weight of the LdPGs concurrently decreased (Fig. 2). This is also true for LdPG **14** which has an average of 36% functionalization with lactose. The sizes of the galectin-3/LdPG aggregates were all the same for 2:1 galectin-3/LdPG mixtures with compounds **11**-**14**. One reasonable rationale for the lack of variance when 2:1 ratios were used is that the concentration of galectin-3 is too low for effective interaction between *N*-terminal domains of LdPG-bound galectin-3. Since all control experiments strongly suggest that interactions between the *N*-terminal domains are critical for controlled aggregate formation (Fig. 3), it is

reasonable that polymer/protein ratios below the threshold for *N*-terminal domain association induce aggregation differently than the observed result using larger excesses of galectin-3.

When lactose functionalization is 35% or higher (LdPGs **11-14**), and the ratio of protein/LdPG is 6:1 or 150:1, then the polymer can evidently bring the galectin-3 proteins close enough together for the *N*-terminal tail domains to overlap. These energetically stabilizing overlaps, combined with specific lectin/carbohydrate binding interactions of the CRD with the lactosides on the LdPGs, allow for reproducible formation of relatively homogeneous galectin-3/LdPG aggregates.

The capacity for galectin-3 to assemble into various oligomeric states, thereby altering its presentation of binding sites, is a widely accepted phenomenon.[38-43] The *N*-terminal domain of galectin-3, which consists of nine Pro/Gly rich collagen-like repeats and a 21 amino acid *N*-terminal segment (protein residues 1-111), has previously been implicated in intermolecular assembly.[40] In solution, galectin-3 frequently presents as a monomer but has been observed to form oligomers at high concentration or in the presence of a multivalent ligand system. In the presence of divalent pentasaccharides featuring terminal *N*-acetyl lactosides, galectin-3 rapidly precipitates as a heterogeneous, disorganized pentameric complex featuring crosslinking interactions with the multivalent saccharide.[38]

With lactose functionalization below 35%, no discernible difference between the aggregation induced by the LdPG and by the unfunctionalized dPGs is observable. The formation of predictably-sized homogenous aggregates is not observed (Fig. 4). These results indicate that there is a threshold of lactose functionalization above which multivalent receptor clustering binding interactions play a significant role in aggregation processes. It is important to note that the aggregates formed by the LdPG systems capable of interacting via specific galectin-3/galactoside binding interactions are smaller and generally more homogeneous than those formed through non-specific binding. These changes are evident when comparing sizes of aggregates initiated with **11-14** to dPG (no lactose functionalization) as shown in Fig. 6 and is expected if specific binding dictates a more orderly formation of aggregates.

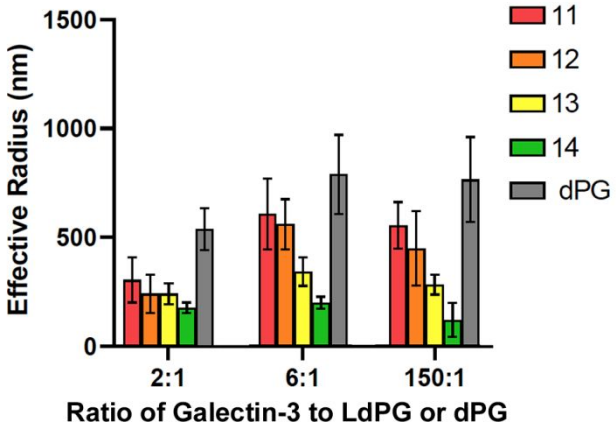


**Fig. 6** Comparison of DLS results for galectin-3/LdPG aggregation using **11-14** to aggregation induced by unfunctionalized dPG.

Control experiments demonstrated that protein/polymer aggregation is dependent on the multivalent nature of the starting materials; aggregation is minimal for monosaccharides (Fig. 2). The effective radii of aggregates observed in the presence of monovalent lactosides are slightly larger than the radius of monomeric galectin-3; presumably some low aggregate associations such as dimers are forming. Monovalent mannose, which does not participate in significant specific binding interactions with the galectin-3 binding pocket, also appears to induce a similarly low level degree of galectin-3 oligomerization. The aggregation that is observed with monomeric lactose, monomeric mannose, and dPGs bearing low densities of lactosides suggests that these materials can enforce low level molecular association even if they are unable to induce more specific aggregate formations that utilize the galectin-3/galactoside binding affinity.

The carbohydrate recognition domain of galectin-3 expressed without the *N*-terminal tail region does not undergo formation of aggregates when introduced to a multivalent glycopolymer (Fig. 3). Aggregation is also not observed when the CRD alone is mixed with monomeric lactoside and mannoside. These critical observations demonstrate that galectin-3 interactions are dependent on the *N*-terminus. Furthermore, the binding interactions that give rise to large irregular aggregates which are indistinguishable from nonspecific binding processes (Fig. 4) must also be reliant on the *N*-terminal domain.

Previous work demonstrated that poly(amidoamine) (PAMAM) glycopolymers functionalized with appropriate carbohydrate ligands formed aggregates when in solution with target receptors.[33, 44, 45] Lactose functionalized PAMAM dendrimers came together with galectin-3 and produced nanometer and micron scale aggregates. These aggregates increased in size as the generation of the dendrimer increased.[33] Unlike the LdPGs reported here, the hydrodynamic radii of the lactose functionalized PAMAM dendrimers increased with increasing molecular weight. Thus, comparison of results for nucleation of galectin-3 aggregation using LdPGs and dendrimers reveals that the hydrodynamic radius of the nucleating polymer (and not necessarily the molecular weight) heavily influences aggregation.

As highlighted in the DLS studies, the interaction of *N*-terminal domains significantly impacted the formation of LdPG-templated protein aggregates. At the highest concentration of LdPG **12**, one would therefore expect the largest amount of binding of galectin-3 to the LdPG during the cellular aggregation assay. With increased binding of the galectin-3 to the LdPG, more opportunities for interactions between *N*-terminal domains should be expected. In turn, improved cellular aggregation is expected to occur, and this was the observed result. At lower concentrations of the LdPG, the binding trend appeared to be more heavily influenced by the number of lactosides presented to the galectin-3 than by the hydrodynamic radius of the LdPG. Thus, LdPG **12** which has a similar hydrodynamic radius to previously studied large dendritic polymers and a carbohydrate loading similar to smaller dendrimers is capable of either inhibiting or enhancing

cancer cellular aggregation depending on the concentration of LdPG used. LdPG **12** is capable of achieving different results in the cellular aggregation assay based on concentration, and this was not easily achievable by glycodendrimers.

Thus, the results described here demonstrate the importance of dPGs for the study of biomedical processes. These studies with lactose functionalized dPGs reveal the critical role of the *N*-terminal domain of galectin-3 in mediating the multivalent aggregation processes responsible for cancer cellular aggregation.

## Conclusions

The lactose functionalized dendritic polyglycerols reported here serve to nucleate the formation of galectin-3/glycopolymer aggregates. Specifically, the lactose functionalized dPGs **11**-**13** nucleate the formation of well-ordered aggregates via a combination of specific protein/carbohydrate interactions and intermolecular overlaps of the N-terminal domains.

These studies have demonstrated a lower limit of lactoside functionalization for effecting the clustering of galectin-3 lectins. When lactoside functionalization is below 35% (LdPGs **15-17**), then protein binding becomes indistinguishable from that induced by unfunctionalized dPGs. Irregular and unpredictable aggregation events cause formation of much less homogeneous protein/polymer aggregates. Control experiments show that associations that are indistinguishable from nonspecific association are localized to the *N*-terminal tail domain and that the *N*-terminal domain is essential for both specific and non-specific aggregate formation. Furthermore, neither monomeric lactose nor mannose initiates aggregation, but the monosaccharides may induce a low level of nonspecific oligomerization through molecular crowding effects.

When galectin-3 proximity supports receptor clustering, then a clear relationship emerges between the size of the glycopolymer and the size of the aggregate that is formed. Lactose functionalized dPGs with larger hydrodynamic radii formed larger aggregates even though their molecular weights were smaller. This reveals the importance of hydrodynamic radius as a guiding principle for the design of polymers for the study of multivalent interactions with proteins and also for the formation of protein/polymer aggregates that may be used to study and to mediate cellular recognition processes.

## Conflicts of interest

There are no conflicts to declare.

## Acknowledgements

NSF 1214134 and the Tamara Joy Henderson Fund are gratefully acknowledged for financial support. NIGMS 62444 provided funds for the purchase of the DLS. R. Haag thanks the SFB 765 of the German Science Foundation (DFG) for financial support.

## References

1. M. Calderon, M. A. Quadir, S. K. Sharma and R. Haag, *Adv. Mater.*, 2010, **22**, 190-218.
2. S. Abbina, S. Vappala, P. Kumar, E. M. J. Siren, C. C. La, U. Abbasi, D. E. Brooks and J. N. Kizhakkedathu, *J. Mat. Chem. B*, 2017, **5**, 9249-9277.
3. M. Jafari, S. Sadat Abolmaali, H. Najafi and A. Mohammad Tamaddon, *Int. J. Pharmaceutics*, 2019, 118959-118959.
4. C. Siegers, M. Biesalski and R. Haag, *Chem.-Eur. J.*, 2004, **10**, 2831-2838.
5. I. N. Kurniasih, J. Keilitz and R. Haag, *Chem. Soc. Rev.*, 2015, **44**, 4145-4164.
6. P. Ray, L. Alhalhooly, A. Ghosh, Y. Choi, S. Banerjee, S. Mallik, S. Banerjee and M. Quadir, *ACS Biomater. Sci. Eng.*, 2019, **5**, 1354-1365.
7. L. Gao, F. Zabihi, S. Ehrmann, S. Hedtrich and R. Haag, *J. Controlled Release*, 2019, **300**, 64-72.
8. K. Pant, C. Neuber, K. Zarschler, J. Wodtke, S. Meister, R. Haag, J. Pietzsch and H. Stephan, *Small*, 2019.
9. M. Mammen, S. K. Choi and G. M. Whitesides, *Angew. Chem., Int. Ed.*, 1998, **37**, 2755-2794.
10. M. J. Cloninger, B. Bilgicer, L. Li, S. L. Mangold, S. T. Phillips and M. L. Wolfenden, *Multivalency in Supramolecular Chemistry: From Molecules to Nanomaterials*, John Wiley & Sons Ltd, Chichester, UK, 2012.
11. R. J. Pieters, *Org. Biomol. Chem.*, 2009, **7**, 2013-2025.
12. L. L. Kiessling, T. Young, T. D. Gruber and K. H. Mortell, *Multivalency in Protein-Carbohydrate Recognition*, Springer-Verlag, Berlin Heidelberg, 2008.
13. J. N. Kizhakkedathu, A. L. Creagh, R. A. Shenoi, N. A. A. Rossi, D. E. Brooks, T. Chan, J. Lam, S. R. Dandepally and C. A. Haynes, *Biomacromolecules*, 2010, **11**, 2567-2575.
14. I. Papp, J. Dernedde, S. Enders, S. B. Riese, T. C. Shiao, R. Roy and R. Haag, *ChemBioChem*, 2011, **12**, 1075-1083.
15. M. H. Staegemann, B. Gitter, J. Dernedde, C. Kuehne, R. Haag and A. Wiehe, *Chem.-Eur. J.*, 2017, **23**, 3918-3930.
16. I. Papp, C. Sieben, A. L. Sisson, J. Kostka, C. Boettcher, K. Ludwig, A. Herrmann and R. Haag, *ChemBioChem*, 2011, **12**, 887-895.
17. M. Ahmed, B. F. L. Lai, J. N. Kizhakkedathu and R. Narain, *Bioconj. Chem.*, 2012, **23**, 1050-1058.
18. D. Haksar, E. de Poel, L. Q. van Ufford, S. Bhatia, R. Haag, J. Beekman and R. J. Pieters, *Bioconj. Chem.*, 2019, **30**, 785-792.
19. J. Dernedde, I. Papp, S. Enders, S. Wedepohl, F. Paulus and R. Haag, *J. Carbohydr. Chem.*, 2011, **30**, 347-360.
20. S. Sciacchitano, L. Lavra, A. Morgante, A. Ulivieri, F. Magi, G. P. De Francesco, C. Bellotti, L. B. Salehi and A. Ricci, *Int. J. Mol. Sci.*, 2018, **19**.
21. P. P. Ruvolo, *Biochim. Biophys. Acta, Mol. Cell Res.*, 2016, **1863**, 427-437.
22. J. Dumic, S. Dabelic and M. Flogel, *Biochim. Biophys. Acta, Gen. Sub.*, 2006, **1760**, 616-635.
23. S. H. Barondes, V. Castronovo, D. N. W. Cooper, R. D. Cummings, K. Drickamer, T. Feizi, M. A. Gitt, J. Hirabayashi, C. Hughes, K. Kasai, H. Leffler, F. T. Liu, R. Lotan, A. M. Mercurio, M. Monsigny, S. Pillai, F. Poirer, A. Raz, P. W. J. Rigby, J. M. Rini and J. L. Wang, *Cell*, 1994, **76**, 597-598.
24. Q. C. Zhao, M. Barclay, J. Hilkens, X. L. Guo, H. Barrow, J. M. Rhodes and L. G. Yu, *Mol. Cancer*, 2010, **9**.
25. Q. C. Zhao, X. L. Guo, G. B. Nash, P. C. Stone, J. Hilkens, J. M. Rhodes and L. G. Yu, *Cancer Res.*, 2009, **69**, 6799-6806.

26. A. K. Michel, P. Nangia-Makker, A. Raz and M. J. Cloninger, *ChemBioChem*, 2014, **15**, 2106-2112.
27. J. H. Ennist, H. R. Termuehlen, S. P. Bernhard, M. S. Fricke and M. J. Cloninger, *Bioconj. Chem.*, 2018, **29**, 4030-4039.
28. P. Xu, J. Y. Yang and P. Kovac, *J. Carbohydr. Chem.*, 2012, **31**, 711-720.
29. A. J. Ross, I. A. Ivanova, M. A. J. Ferguson and A. V. Nikolaev, *J. Chem. Soc., Perkin Trans. 1*, 2001, 72-81.
30. K. Anraku, S. Sato, N. T. Jacob, L. M. Eubanks, B. A. Ellis and K. D. Janda, *Org. Biomol. Chem.*, 2017, **15**, 2979-2992.
31. M. Abellan-Flos, M. Tanc, C. T. Supuran and S. P. Vincent, *J. Enzyme Inhib. Med. Chem.*, 2016, **31**, 946-952.
32. I. Papp, J. Dernedde, S. Enders and R. Haag, *Chem. Commun.*, 2008, 5851-5853.
33. C. K. Goodman, M. L. Wolfenden, P. Nangia-Makker, A. K. Michel, A. Raz and M. J. Cloninger, *Beilstein J. Org. Chem.*, 2014, **10**, 1570-1577.
34. A. Sunder, R. Hanselmann, H. Frey and R. Mulhaupt, *Macromolecules*, 1999, **32**, 4240-4246.
35. H. C. Kolb and K. B. Sharpless, *Drug Disc. Today*, 2003, **8**, 1128-1137.
36. A. Lederer, W. Burchard, T. Hartmann, J. S. Haataja, N. Houbenov, A. Janke, P. Friedel, R. Schweins and P. Lindner, *Angew. Chem. Int. Ed.*, 2015, **54**, 12578-12583.
37. S. Shahid, I. Hasan, F. Ahmad, M. I. Hassan and A. Islam, *Biomolecules*, 2019, **9**.
38. N. Ahmad, H. J. Gabius, S. Andre, H. Kaltner, S. Sabesan, R. Roy, B. C. Liu, F. Macaluso and C. F. Brewer, *J. Biol. Chem.*, 2004, **279**, 10841-10847.
39. A. Flores-Ibarra, S. Vertesy, F. J. Medrano, H.-J. Gabius and A. Romero, *Sci. Rep.*, 2018, **8**.
40. A. U. Newlaczyl and L. G. Yu, *Cancer Lett.*, 2011, **313**, 123-128.
41. J. Ochieng, D. Platt, L. Tait, V. Hogan, T. Raz, P. Carmi and A. Raz, *Biochemistry*, 1993, **32**, 4455-4460.
42. S. M. Massa, D. N. W. Cooper, H. Leffler and S. H. Barondes, *Biochemistry*, 1993, **32**, 260-267.
43. D. K. Hsu, R. I. Zuberi and F. T. Liu, *J. Biol. Chem.*, 1992, **267**, 14167-14174.
44. J. M. Cousin and M. J. Cloninger, *Beilstein J. Org. Chem.*, 2015, **11**, 739-747.
45. K. H. Schlick, C. K. Lange, G. D. Gillispie and M. J. Cloninger, *J. Am. Chem. Soc.*, 2009, **131**, 16608-16609.

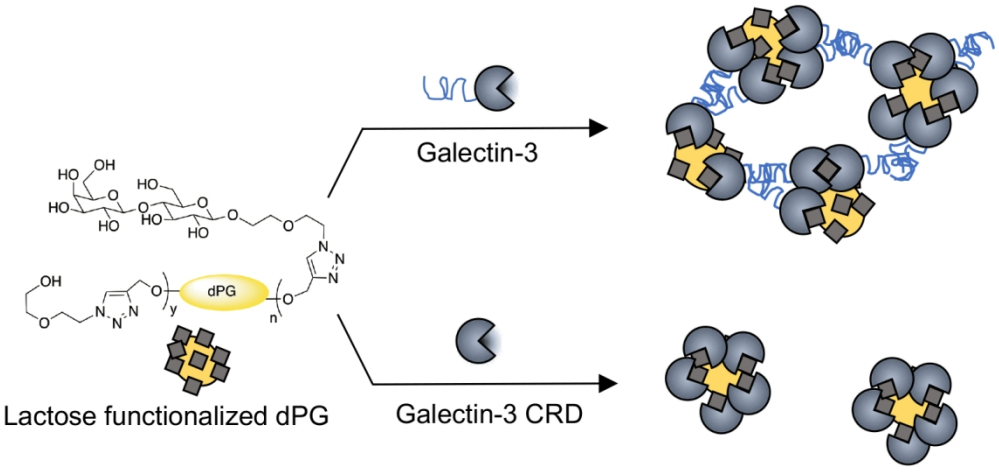


133x61mm (300 x 300 DPI)